Supporting Information

Immobilization of a chiral rhodium catalyst on carbon nanotubes via non-covalent interactions for heterogeneous asymmetric hydrogenation

Zinnia Arora,[a,b] Vasile I. Pârvulescu,[b] Karine Philippot,[a] Jérôme Durand,[a] and Maryse Gouygou*[a]

[a] Laboratoire de Chimie de Coordination du CNRS, Université de Toulouse, UPS, Toulouse-INP, 205 route de Narbonne, BP 44099, F-31077 Toulouse Cedex 4, France
[b] Department of Organic Chemistry, Biochemistry and Catalysis, University of Bucharest, 4-12 Regina Elisabeta Avenue, S3, 030018, Bucharest, Romania
* Corresponding author: maryse.gouygou@lcc-toulouse.fr

Table of Contents

1. NMR Spectrum of the (*2S,4S*)-PPM-pyrene ligand

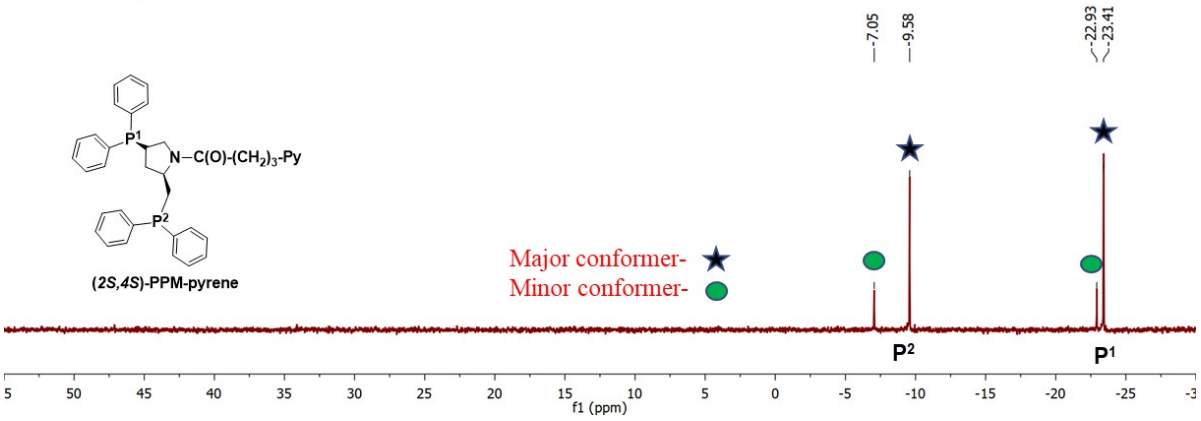

Figure S1: $^{31}P\{^{1}H\}$ NMR spectrum of the (*2S,4S*)-PPM-pyrene ligand.

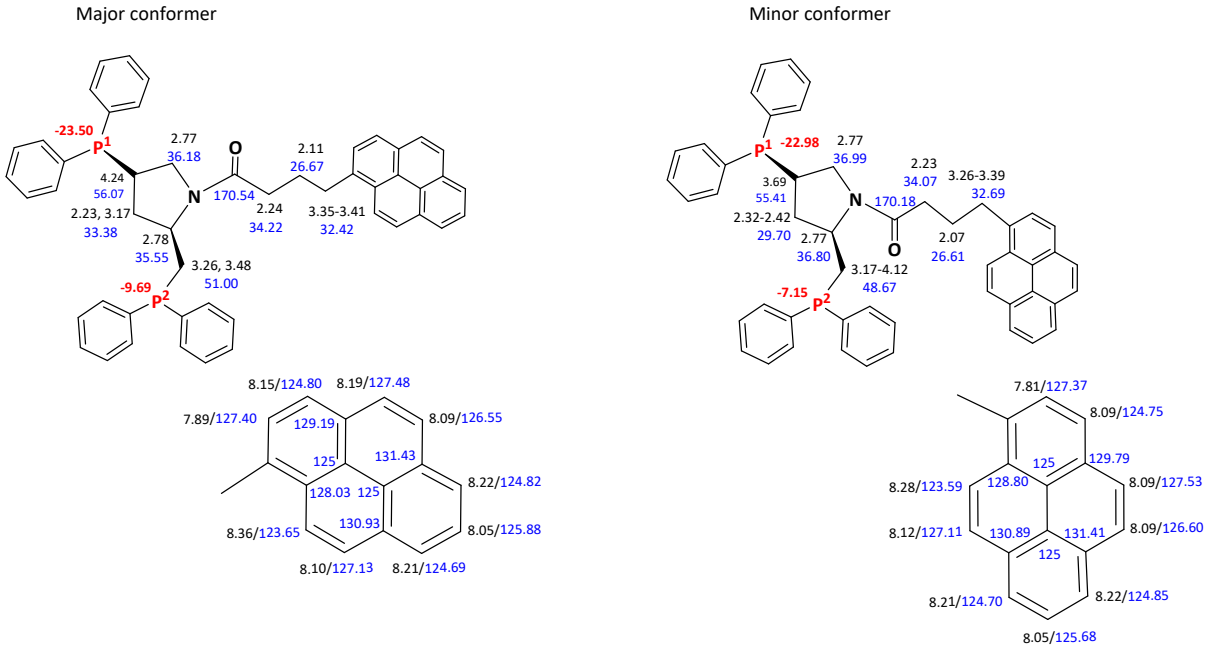

Figure S2: ^{1}H, ^{31}P, and ^{13}C-chemical shifts of the (*2S,4S*)-PPM-pyrene ligand. Attribution made by ^{1}H, $^{1}H\{^{31}P\}$ select and broadband, $^{13}C\{^{1}H\}$, $^{13}C\{^{1}H\},\{^{31}P\}$ COSY, HSQC, HMBC ROESY, HMQC ^{1}H-^{31}P on a Bruker Avance NEO 600. The majority of the protons and carbons of each conformer, including those of the pyrene group were assigned except the protons and carbons of the phenyl groups which are too overlapping to be unambiguously assigned.

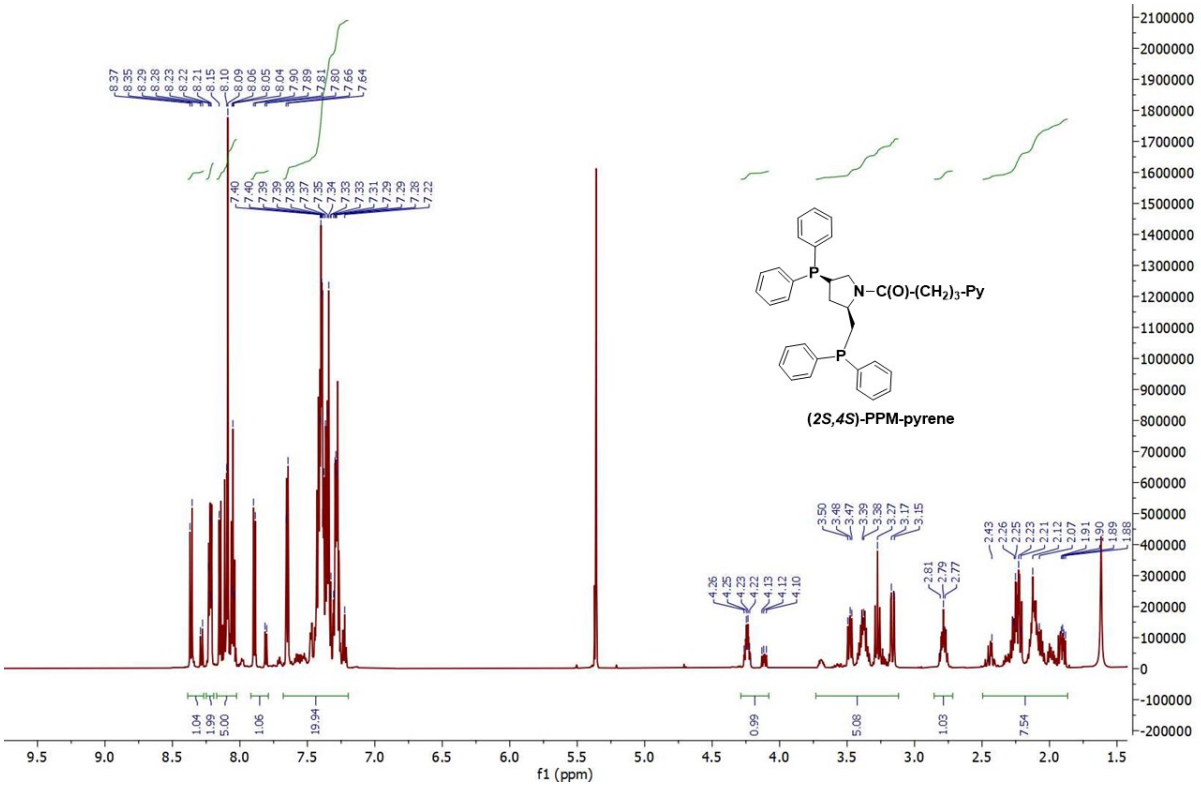

Figure S3: ^{1}H NMR spectrum of the (*2S,4S*)-PPM-pyrene ligand.

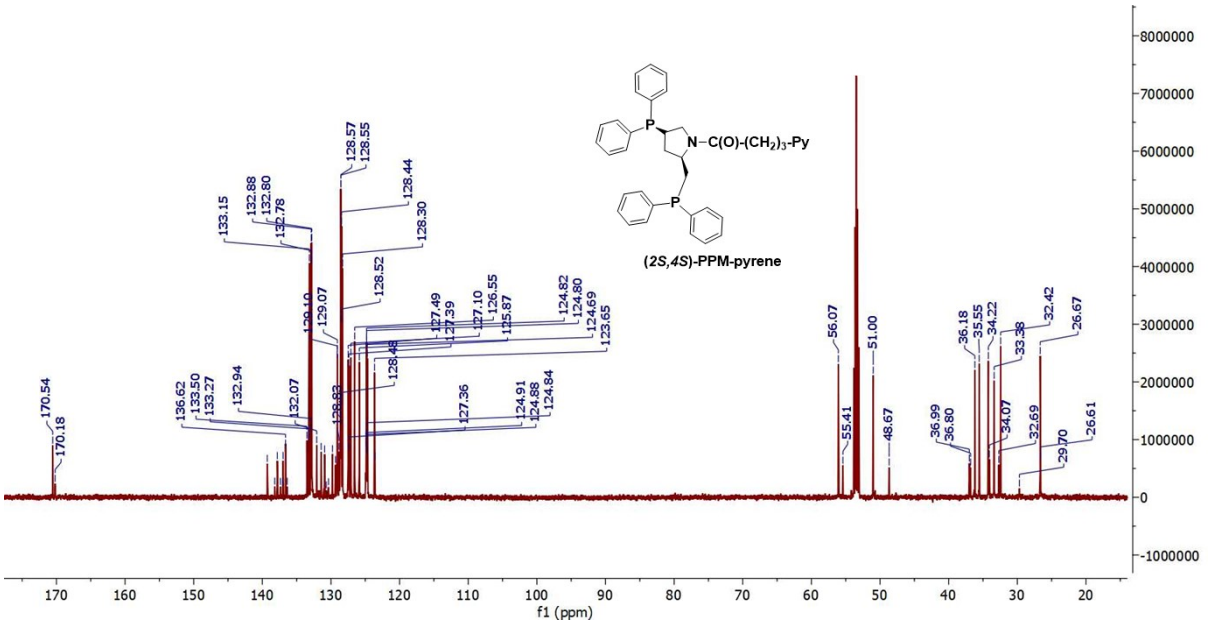

Figure S4: ^{13}C NMR spectrum of the (*2S,4S*)-PPM-pyrene ligand.

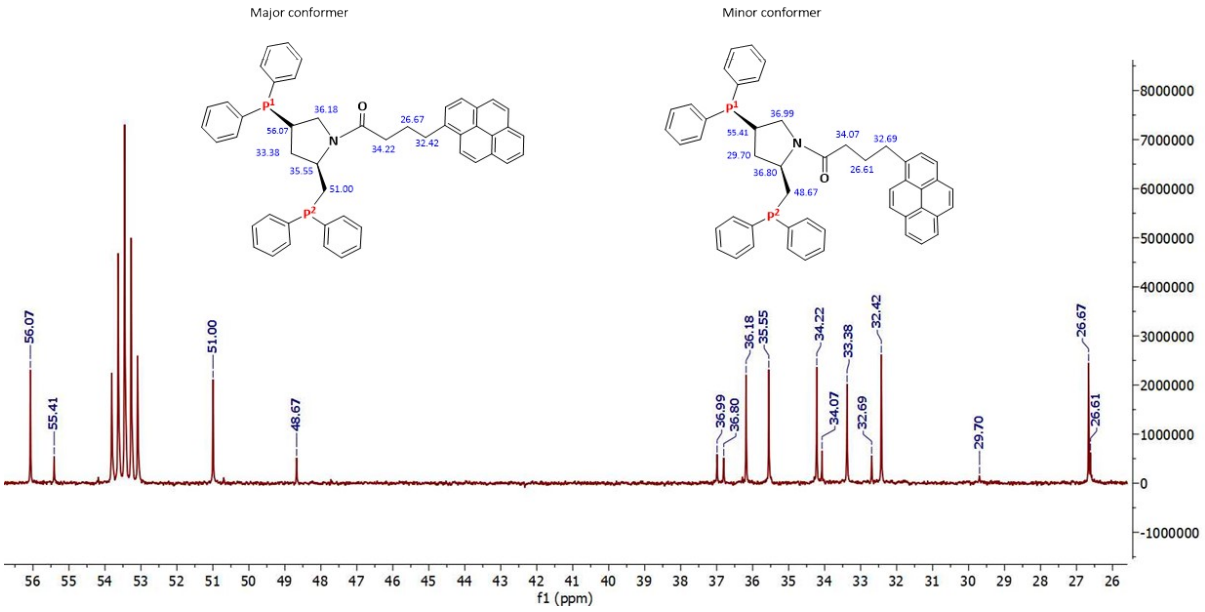

Figure S5: Zoom spectrum of aliphatic carbons of the (*2S,4S*)-PPM-pyrene ligand.

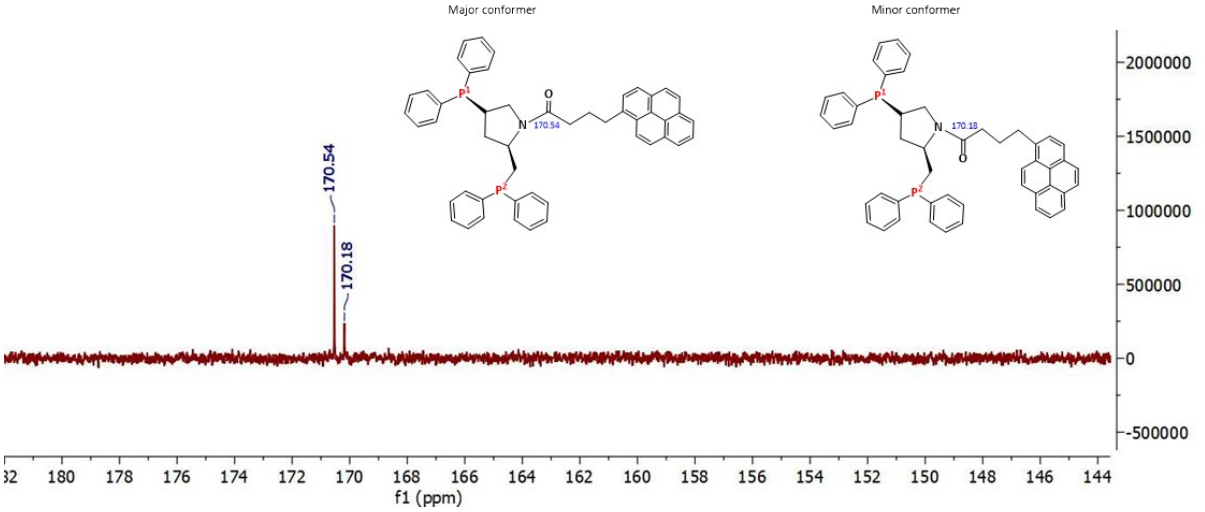

Figure S6: Zoom spectrum of carbonyl carbons of the (*2S,4S*)-PPM-pyrene ligand.

2. Comparison of $^{31}P\{^{1}H\}$ NMR data of (*2S,4S*)-PPM-pyrene ligand and [Rh(COD)((*2S,4S*)-PPM-pyrene)]BF_4 complex.

Figure S7: $^{31}P\{^{1}H\}$ NMR spectra of (*2S,4S*)-PPM-pyrene ligand (bottom, red) and [Rh(COD)((2*S,4S*)-PPM-pyrene)]BF_4 complex (top, blue).

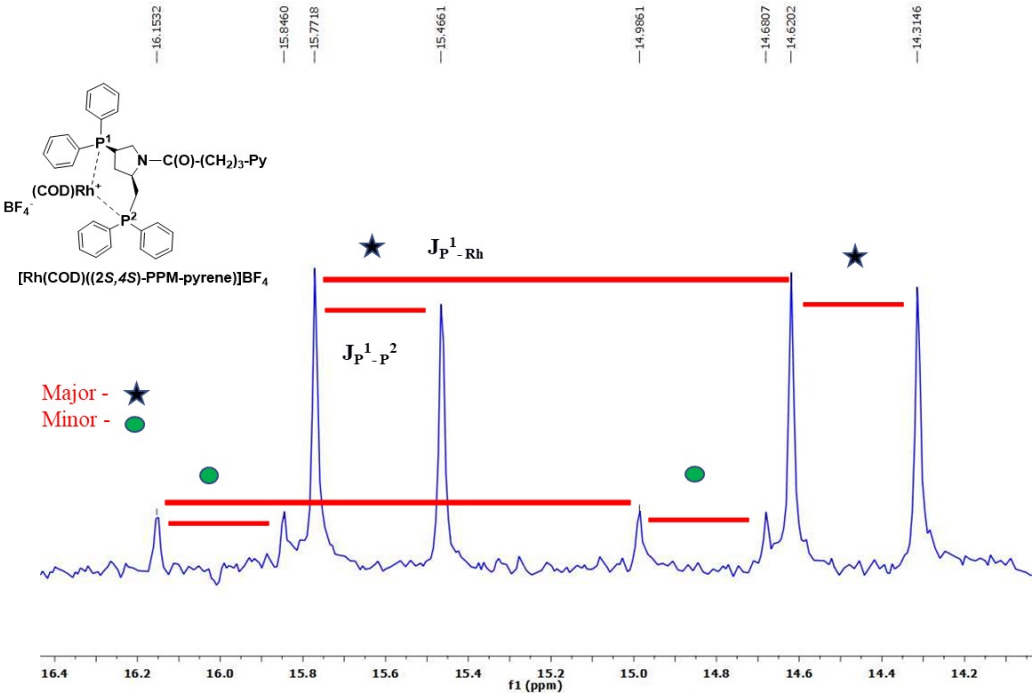

Figure S8: Zoom of $^{31}P\{^{1}H\}$ spectrum of the **[Rh(COD)((*2S,4S*)-PPM-pyrene)]BF_4** complex showing the couplings of P^1 with Rh and P^2 in the major and minor isomers.

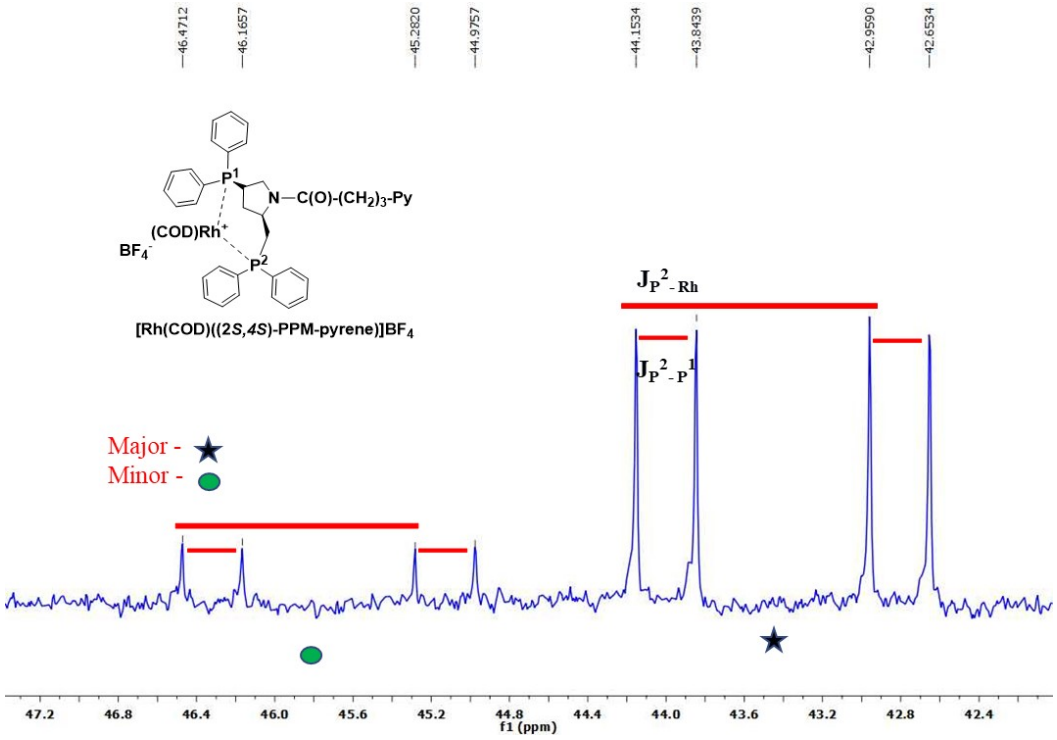

Figure S9: Zoom of $^{31}P\{^{1}H\}$ spectrum of the **[Rh(COD)((*2S,4S*)-PPM-pyrene)]BF_4** complex showing the couplings P^2 with Rh and P^1 in the major and minor isomers.

3. Immobilization of [Rh(COD)((2*S,4S*)-PPM-pyrene)]BF_4 *via* non-covalent π-π interaction

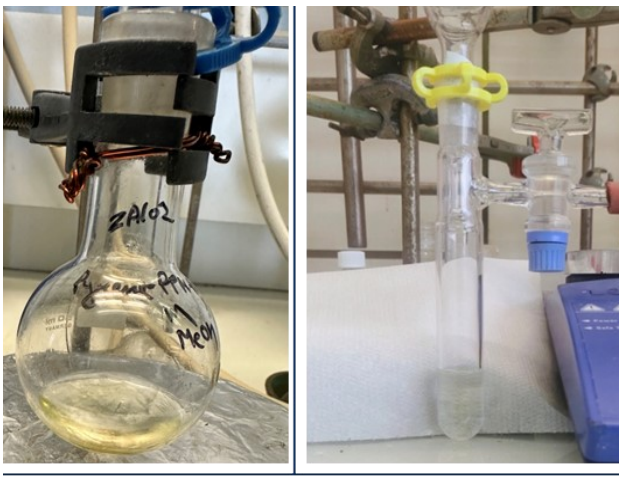

Figure S10: The adsorption of chiral **complex Rh** onto CNTs in MeOH: homogeneous complex solution (left), and the filtrate after immobilization of complex on CNTs (right).

4. FTIR spectra of CNTs and CNT@complex Rh.

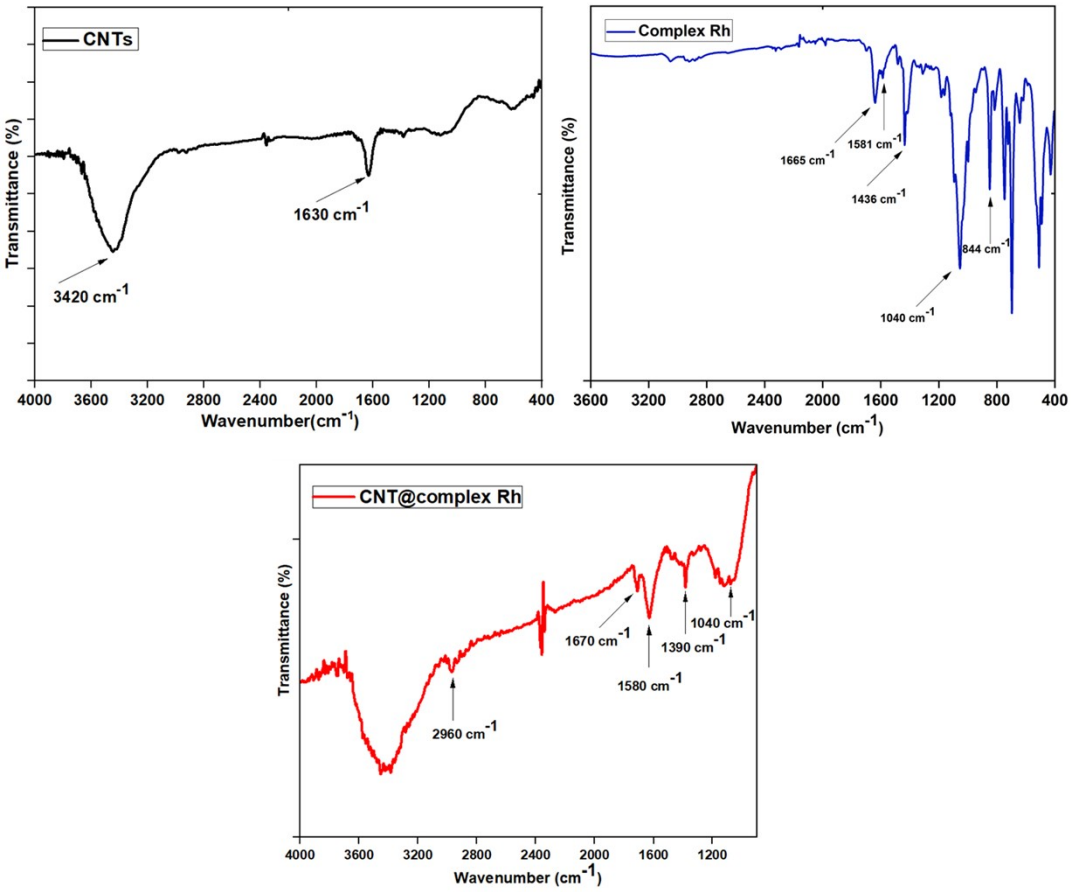

Figure S11: FTIR spectra of the CNTs and CNT@complex Rh.

5. Raman spectra of the CNTs and CNT@complex Rh.

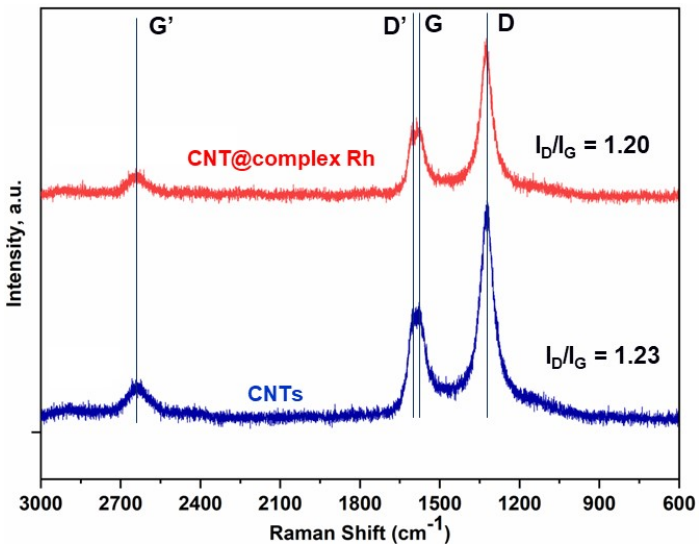

Figure S12: Raman spectra of the **CNTs (blue)** and **CNT@complex Rh (red)**.

6. N_2 adsorption-desorption isotherms of CNTs and CNT@complex Rh

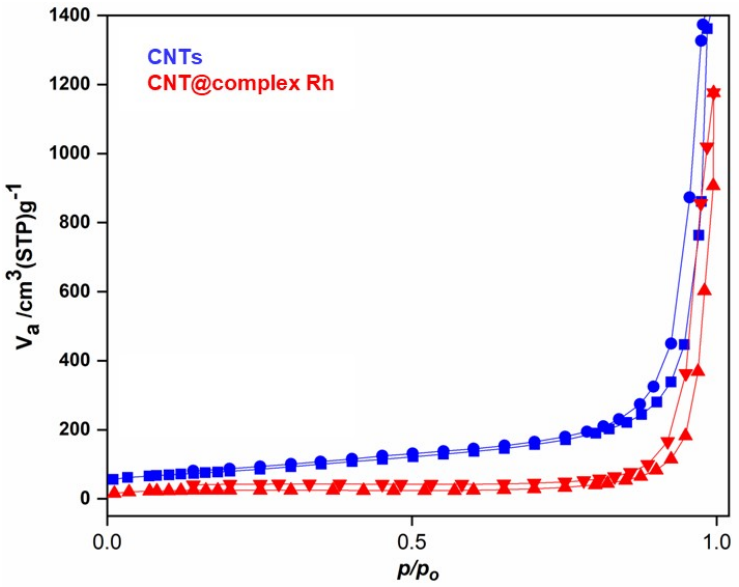

Figure S13: N_2 adsorption-desorption isotherms of **CNTs** (blue) and **CNT@complex Rh** (red).

7. XPS data of the fresh CNT@complex Rh

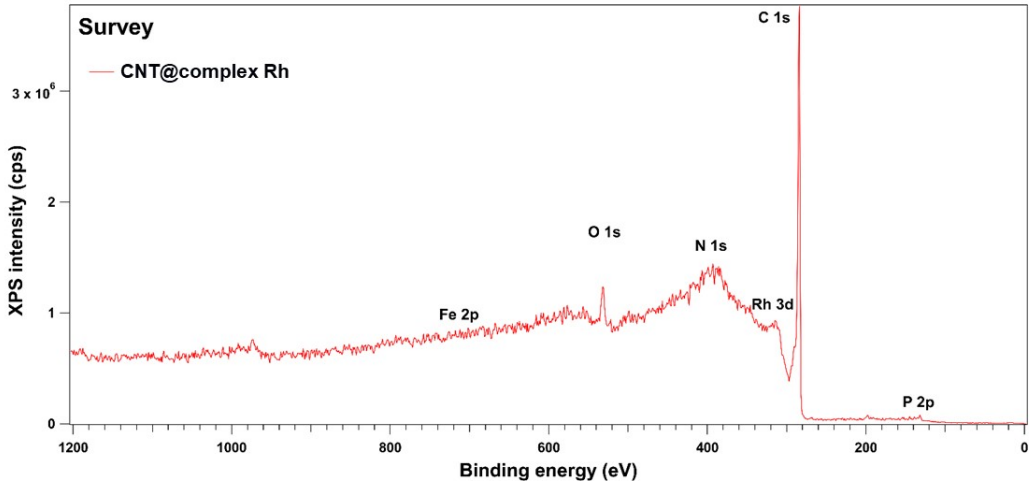

Figure S14: XPS survey of the elements in fresh **CNT@complex Rh**.

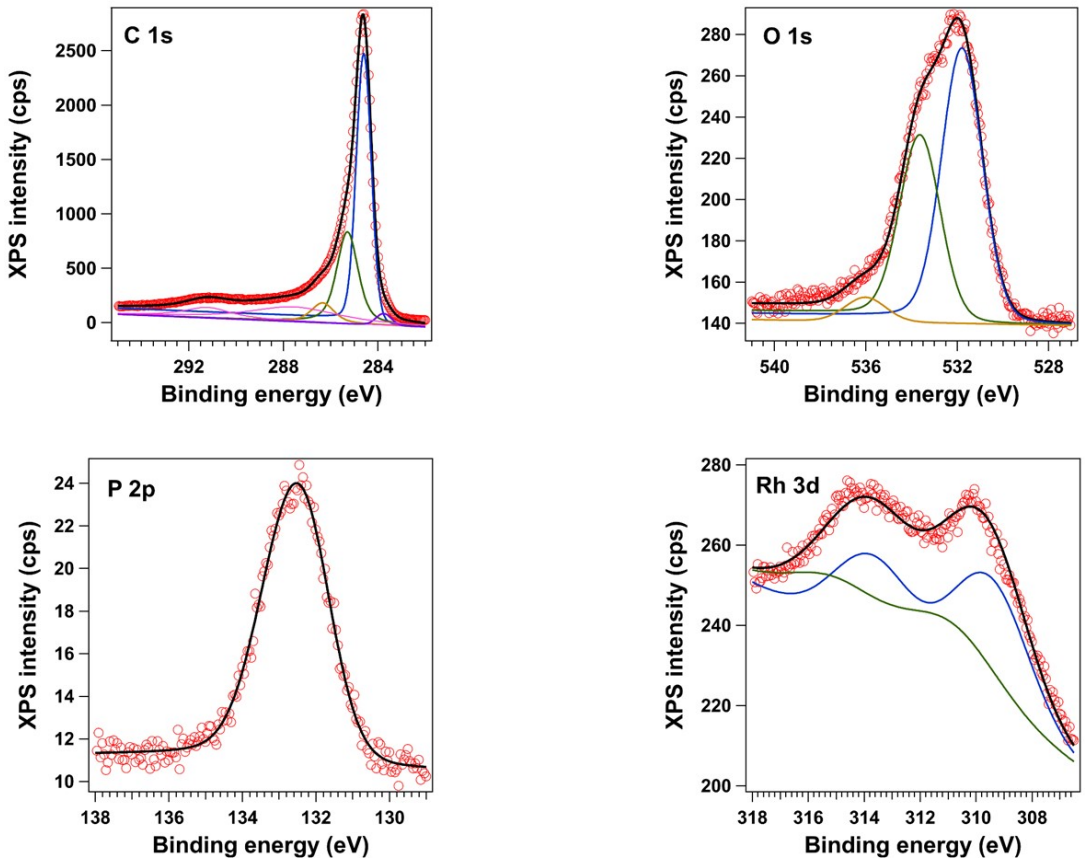

Figure S15: XPS analysis of the elements present in **CNT@complex Rh**. (red: experimental data, black: fitting, blue and green: deconvolution)**.**

Table S1: XPS binding energies and Rh/P atomic ratio for the CNT@complex Rh.

	Binding energy (eV)			
Catalyst	O1s	C1s	P2p	Rh3d
CNT@complex Rh	531.7 533.3 536.0	284.8 285.3 286.3 287 290.8	132.3	309.6 + 313.8 310.5 + 315.0
Rh/P atomic ratio				
		XPS value		Theoretical value
CNT@complex Rh		0.52		0.50

8. GC analysis of catalysis by CNT@complex Rh.

Table S2: GC analysis of catalysis result for the enantioselective hydrogenation of dimethyl itaconate by CNT-immobilized Rh complex (entry 3 of Table 1).

Software Version	: 6.3.2.0646	Date	: 2/25/2022 10:41:45 AM
Operator	: TCPROCESS	Sample Name	:
Sample Number	:	Study	:
AutoSampler	: NONE	Rack/Vial	: 0/0
Instrument Name	: CLARUS 580	Channel	: A
Instrument Serial #	: 580S12101703	A/D mV Range	: 1000
Delay Time	: 0.00 min	End Time	: 30.00 min
Sampling Rate	: 12.5000 pts/s		
Sample Volume	: 1.000000 ul	Area Reject	: 0.000000
Sample Amount	: 1.0000	Dilution Factor	: 1.00
Data Acquisition Time	: 2/23/2022 11:45:32 AM	Cycle	: 1

Raw Data File : C:\Clarus580\DATA\Zinnia\ZA79 _90.raw
Result File : C:\Clarus580\DATA\Zinnia\ZA79 _90.rst [Editing in Progress]
Inst Method : C:\Clarus580\METHODE\Laurent\Methode colonne chirale Maryse fev2022 Modif test from C:\Clarus580\DATA\Zinnia\ZA79 _90.raw
Proc Method : C:\Clarus580\METHODE\Laurent\Methode colonne chirale Maryse fev2022 Modif test from C:\Clarus580\DATA\Zinnia\ZA79 _90.rst [Editing in Progress]
Calib Method : C:\Clarus580\METHODE\Laurent\Methode colonne chirale Maryse fev2022 Modif test from C:\Clarus580\DATA\Zinnia\ZA79 _90.rst [Editing in Progress]
Report Format File: C:\Clarus580\METHODE\Laurent\Methode colonne chirale Maryse fev2022 Modif test.rpt
Sequence File : C:\AUTOSYSTEM XL\SEQUENCE\ZA79 _90.seq

DEFAULT REPORT

Peak #	Time [min]	Area [µV·s]	Height [µV]	Area [%]	Norm. Area [%]	BL	Area/Height [s]
1	0.764	54071.02	46441.07	0.90	0.90	BV	1.1643
2	0.806	393901.29	106733.85	6.57	6.57	VV	3.6905
3	0.853	85904.45	79489.69	1.43	1.43	VV	1.0807
4	0.878	156542.94	84521.51	2.61	2.61	VV	1.8521
5	0.903	29653.46	61845.76	0.49	0.49	VV	0.4795
6	0.920	4861470.14	988672.15	81.11	81.11	VE	4.9172
7	1.103	4043.73	1526.98	0.07	0.07	EV	2.6482
8	1.204	189.42	208.49	0.00	0.00	VB	0.9086
9	1.314	450.87	240.97	0.01	0.01	BV	1.8710
10	1.386	109.23	73.54	0.00	0.00	VB	1.4853
11	1.705	591.21	228.39	0.01	0.01	BB	2.5885
12	1.867	240.80	88.35	0.00	0.00	BB	2.7257
13	2.051	709.10	244.46	0.01	0.01	BB	2.9006
14	2.161	3433.46	1929.70	0.06	0.06	BV	1.7793
15	2.249	162.31	76.50	0.00	0.00	VB	2.1217
16	4.656	218.19	73.41	0.00	0.00	BB	2.9722
17	7.812	603.57	127.21	0.01	0.01	BV	4.7447
18	7.945	76427.56	11037.13	1.28	1.28	VV	6.9246
19	8.334	37390.11	4998.38	0.62	0.62	VB	7.4804
20	11.544	285505.02	29549.25	4.76	4.76	BE	9.6620
21	11.941	1801.68	222.44	0.03	0.03	EB	8.0995
22	12.050	35.52	72.10	0.00	0.00	BB	0.4926
23	12.067	60.02	78.61	0.00	0.00	BB	0.7635
24	12.092	55.78	82.34	0.00	0.00	BB	0.6774
25	12.112	38.09	67.90	0.00	0.00	BB	0.5610
		5993608.95	1.42e+06	100.00	100.00		

The retention times for the produced methyl succinate were 7.9 and 8.3 min for the (*S*) and (*R*) forms, respectively, and 11.5 min for dimethyl itaconate.

R = 0.62
S = 1.28
Reactant = 4.76

$$\% \, Conversion = 100 - \frac{Area \, of \, Reactant}{Total \, area} * 100$$

$$\% \, Conversion = 100 - \frac{4.76}{4.76 + 1.28 + 0.62} * 100$$

$$\% \, Conversion = 100 - \frac{4.76}{4.76 + 1.28 + 0.62} * 100$$

$$\% \, Conversion = 29$$

$R = 0.62$
$S = 1.28$

$$\% \, ee = \frac{|R - S|}{R + S} * 100$$

$$\% \, ee = \frac{|0.62 - 1.28|}{0.62 + 1.28} * 100$$

$$\% \, ee = 34 \, (S)$$

9. FTIR spectra of fresh and spent CNT@complex Rh catalyst.

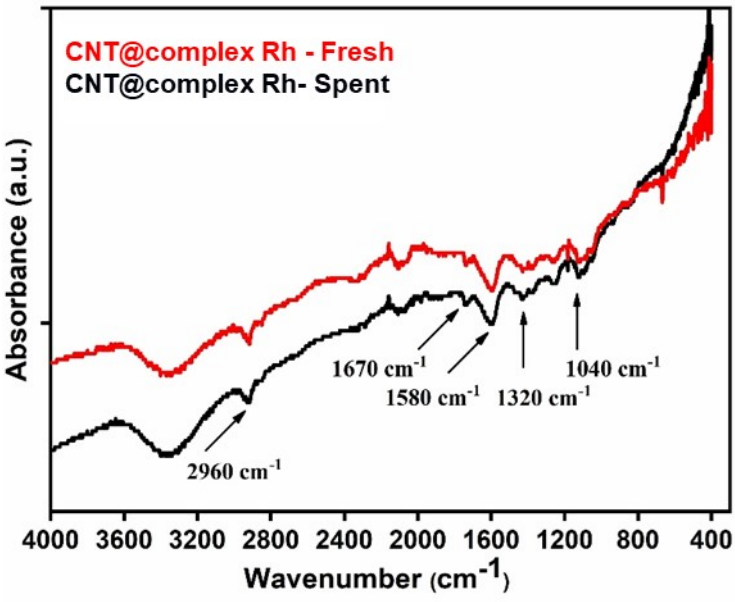

Figure S16: FTIR spectra of fresh (red) and spent (black) **CNT@complex Rh** catalyst.

10. XPS spectra of Rh for the fresh and spent of CNT@complex Rh.

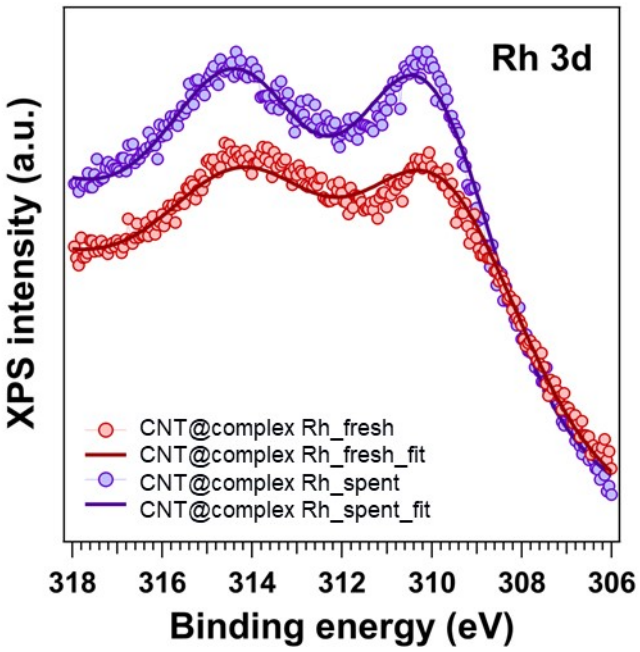

Figure S17: XPS spectra of Rh for the fresh (red) and spent (violet) **CNT@complex Rh**.